JOURNAL OF GEOPHYSICAL RESEARCH, VOL. 101, NO. D1, PAGES 1961–1974, JANUARY 20, 1996

Walker circulation and tropical upper tropospheric water vapor

Reginald E. Newell and Yong Zhu
Massachusetts Institute of Technology, Cambridge

Edward V. Browell
NASA Langley Research Center, Hampton, Virginia

William G. Read and Joe W. Waters
Jet Propulsion Laboratory, California Institute of Technology, Pasadena

Abstract. Maps of the boundary layer divergent wind component derived from velocity potential for two 35-day periods in 1991 and 1994 exhibit a pattern of convergence in the lower levels in the tropical western Pacific, following the Sun between hemispheres, and divergence in the eastern Pacific, these two features agreeing with schematics of the Walker circulation. Vertical motion maps show rising motion in the western Pacific and sinking motion in the eastern Pacific; water vapor maps derived from the microwave limb sounder on the Upper Atmosphere Research Satellite show a similar picture with moist plumes evident at 215 hPa in rising regions and dryness in sinking regions. While these three indicators of vertical motion are internally consistent and fit with accepted views of the Walker circulation, it is shown that there is not equally clear evidence that the eastern and western regions are directly linked by horizontal motions, particularly in the upper troposphere. Mass flux studies based on the divergent winds show that the southeastern Pacific anticyclonic region is fed by upper tropospheric inflow from all sides; in October 1991 the inflow from the west, east, south, and north contributed almost equally, while in February 1994 the inflow from the west was the largest contribution, but flow across the eastern and southern boundaries was also important. The water vapor maps suggest that a substantial fraction of air in the upper troposphere to the west of South America originates over the continent. Lidar measurements of cirrus show good evidence of diverging flow into the northern hemisphere from the rising motion in the west Pacific near 10°S during February 1994. The situation in the southeastern Pacific cell in October 1991 is somewhat analogous to that in the northwestern Pacific cell in February 1994 in that flow from a nearby landmass is entrained into the circulation. From daily water vapor maps coupled with potential vorticity maps and cross sections, it is suggested that direct exchange between the stratosphere and the troposphere in the form of almost vertical plumes may occur in subsiding regions in the tropics.

Introduction

The Walker circulation is the name given to a supposed toroidal atmospheric circulation in the tropical Pacific which involves rising motion in the west, sinking motion in the east, a westward flow at low levels, and an eastward flow in the upper troposphere. Suggestions of a toroidal circulation were made by *Troup* [1965], who was studying Walker's Southern Oscillation and who deduced the circulation from height data given by *Heastie and Stephenson* [1960] and from temperature differences in the free troposphere between Darwin and Lima. *Bjerknes* [1969] deduced a similar toroidal circulation from the data of Heastie and Stephenson and stressed its compatibility with sea surface temperature patterns; he christened it the "Walker circulation." Climatological wind velocity data have been used to support the existence of such a toroidal circulation, but some of these distributions used deviations from zonal mean zonal wind velocity [e.g., *Newell et al.*, 1974]. The rising arm of the circulation moves toward the east, often reaching the date line, when sea surface temperatures are higher than average in the eastern equato-

Paper number 95JD02275.
0148-0227/96/95JD-02275$05.00

rial Pacific during the El Niño-Southern Oscillation cycle. Observations and the theory behind the processes have been reviewed by *Philander* [1990]. There is also another linkage, often portrayed as a toroidal circulation, between the South American continent and the eastern tropical Pacific, and there is much interest in how this continental air interacts photochemically with the cleaner air over the tropical Pacific. A similar problem has recently been investigated experimentally for air passing from the Asian continent to the western Pacific [*Hoell et al.*, this issue].

The purpose here is to compare data on atmospheric circulation parameters, upper tropospheric water vapor, and lidar scattering by cirrus to see how the three fit together in the context of the Walker circulation and to define some of the requirements for an aircraft field experiment to check the interaction between continental, marine, and stratospheric air in the southeastern Pacific region. Two periods (in different seasons) were selected for the data comparison: September 17 to October 22, 1991, and February 7 to March 14, 1994. These were the periods of the NASA Global Tropospheric Experiment, Pacific Exploratory Mission West (PEMW) during which the NASA DC-8 was deployed to the West Pacific for sampling a number of atmospheric trace constituents [*Hoell et al.*, this issue]; hereinafter, the two periods will be termed PEMWA and PEMWB respectively. The Upper Atmosphere Research Satellite (UARS) was measuring water vapor in the upper troposphere with the microwave limb sounder (MLS) instrument during both of these periods [*Barath et al.*, 1993]. We have reported elsewhere a comparison between the water vapor measured in situ by the DC-8 and that measured by MLS for the upper troposphere in the PEMWA period [*Newell et al.*, this issue].

Divergent Wind and Water Vapor Patterns in the Walker Circulation

The basic circulation data used was 12-hour grid point data from the European Center for Medium-Range Weather Forecasts (ECMWF) model T213 (corresponding to a horizontal resolution of about 189 km); the data include geopotential, three wind velocity components, temperature, and relative humidity. Helmholtz showed that a vector function can be expressed as the sum of two others, one divergenceless and one irrotational (see, for example, *Weatherburn* [1951]. With this concept the horizontal wind velocity may be written:

$$\underset{\sim}{V} = -\nabla\chi + k \times \nabla\phi = \underset{\sim}{V}_d + \underset{\sim}{V}_r \qquad (1)$$

where χ is a velocity potential and ϕ a stream function [see *Bluestein*, 1993]. Taking the divergence and curl of this equation in turn yields

$$\nabla \cdot \underset{\sim}{V} = -\nabla^2\chi \qquad (2)$$

$$\nabla \times \underset{\sim}{V} = \nabla^2\phi \qquad (3)$$

Solving the two Laplacians for χ and ϕ then enables V to be written in terms of its two components. The irrotational wind component, the first term in equation (1), is obtained directly from the gradient of the velocity potential and is usually referred to as the divergent wind. The rotational component, which is divergenceless, is in the free troposphere equivalent to the geostrophic wind. In solving equations (2) and (3) for χ and ϕ, no boundary conditions were involved, as a complete global data set was used. Maps of χ and ϕ at 1000 and 200 hPa and the associated wind components are given for PEMWA in Figures 1a and 1b. At 1000 hPa, substantial inflow occurs in the west, near 15°N, 120-140°E and in the east near Panama. In addition, there is convergence along 10°N in the central Pacific, in a region stretching southeastward from about 15°N, 150°E to about 15°S, 140°W, the so-called South Pacific Convergence Zone (SPCZ), and along 155°W in the North Pacific. Convergence occurs in the same regions up to about 500 hPa. At 1000 hPa, divergence occurs off the west coasts of the Americas; off North America the divergent center diminishes fairly rapidly with altitude and has disappeared by 500 hPa, while off South America, there is still a strong center at higher levels, but it has shifted toward the west by 500 hPa. Divergence also occurs near the date line at 35°N and off the east and west coasts of Australia. At 200 hPa, divergent circulations

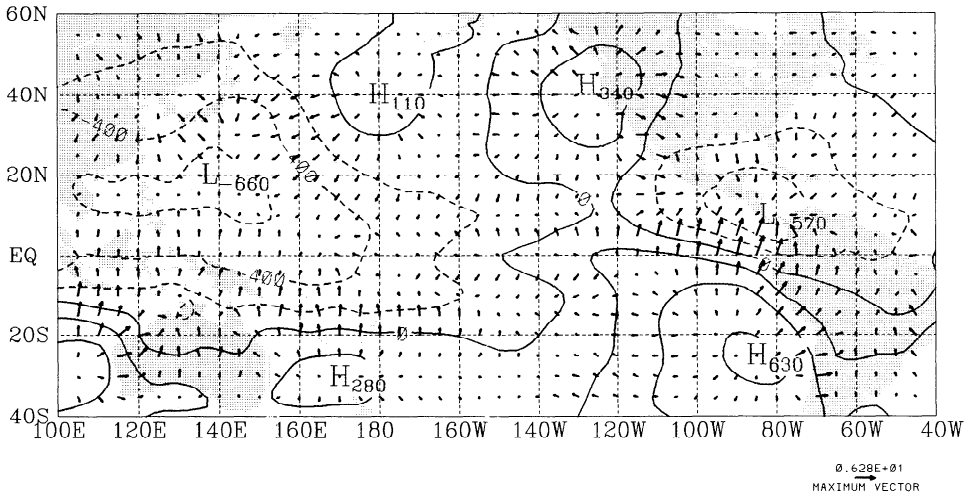

Figure 1a. Mean Pacific Exploratory Mission A (PEMWA) velocity potential (units, 10^4 m^2 s^{-1}) and divergent wind (units, ms^{-1}) at 1000 hPa.

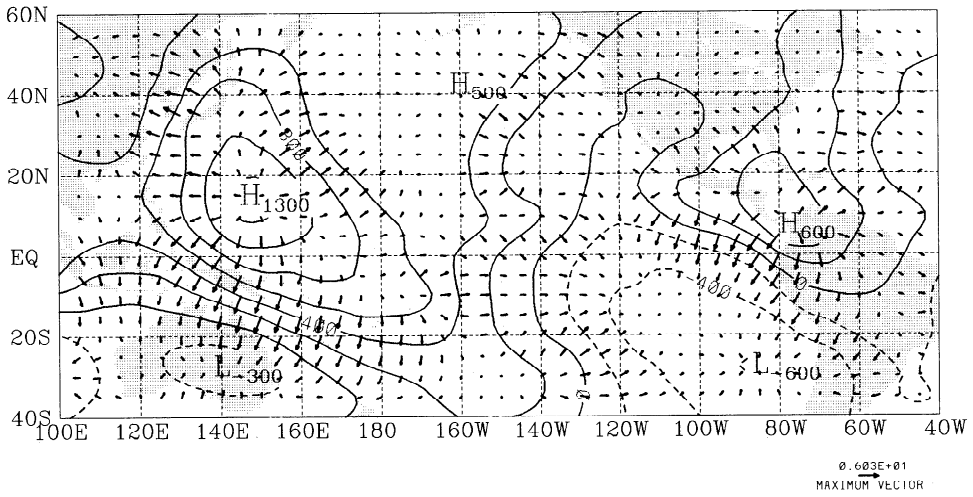

Figure 1b. Mean PEMWA velocity potential (units, 10^4 m^2 s^{-1}) and divergent wind (units, ms^{-1}) at 200 hPa.

compensating these lower-level convergences occur in the western and central Pacific at 10°N, over the SPCZ region and over Panama, while over the southeastern Pacific and over Australia, there is strong convergence. Somewhat weaker convergence occurs over the west coast of North America and the central North Pacific (near 180°W). There is also weak divergence along 160°W in the central North Pacific.

For the PEMWB period, shown in Figures 2a and 2b at 1000 and 200 hPa, the centers of convergence at 1000 hPa are at about 10°S, 150°E and over the Amazon Basin. The SPCZ is almost aligned west-east from 10°S, 150°E, while the convergence line in the central Pacific is at about 5°N, compared with 10°N in PEMWA. There is also a weak convergence region in the North Pacific near 170°E. As before, there are divergent regions off the west coasts of the Americas and, in addition, a small region over the Sea of Japan. The convergent regions have almost completely disappeared by 500 hPa (not shown) and the divergent region over the Southeast Pacific has been replaced by convergence. A divergent region exists south of the equator at about 160°W. At 200 hPa there is strong divergence over the upwelling regions at 10°S, 100°-160°E, and somewhat weaker regions over the North Pacific and South America. There is strong convergence off the west coast of South America extending northward over into the South Atlantic and another region over China. There is also a weak divergent region centered at about 5°N, from 160°W eastward. The vertical motion patterns at 300 hPa (Figures 3a and 3b) fit in with these convergent-divergent patterns. From the divergent wind components and the vertical velocity maps, there is substantial evidence for the vertical components of the Walker circulation with the rising arm in the western Pacific following the Sun between hemispheres, while the sinking arm off South America stays relatively fixed. Because of this difference, at 100°W, 5°S the surface level airflow always has a component from the south, whereas at 140°E, 5°N there is an alternation between northerly flow in the early part of the year and southerly flow in the latter part.

Preliminary water vapor values deduced from MLS on UARS are shown for the PEMWA period in Figures 4a and 4b for 215 and 147 hPa. Both levels show plumes of high

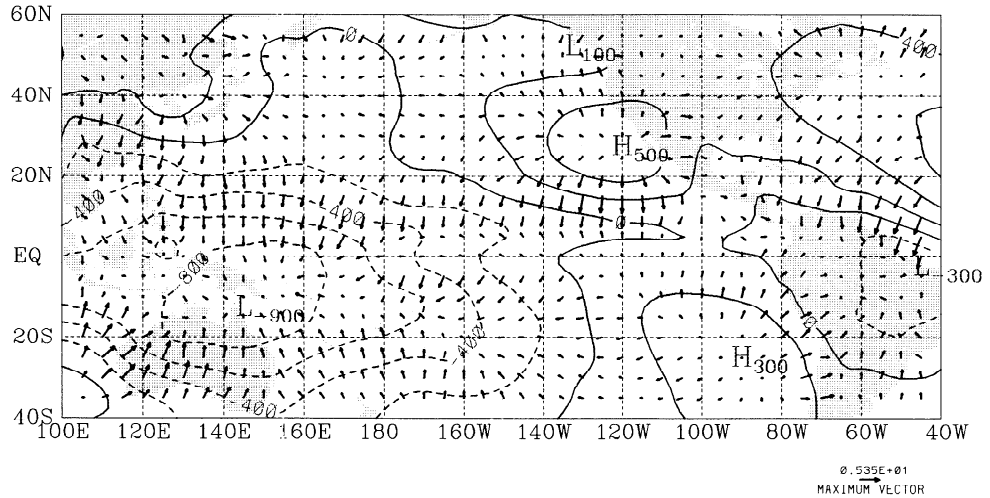

Figure 2a. Mean PEMWB velocity potential (units, 10^4 m^2 s^{-1}) and divergent wind (units, ms^{-1}) at 1000 hPa.

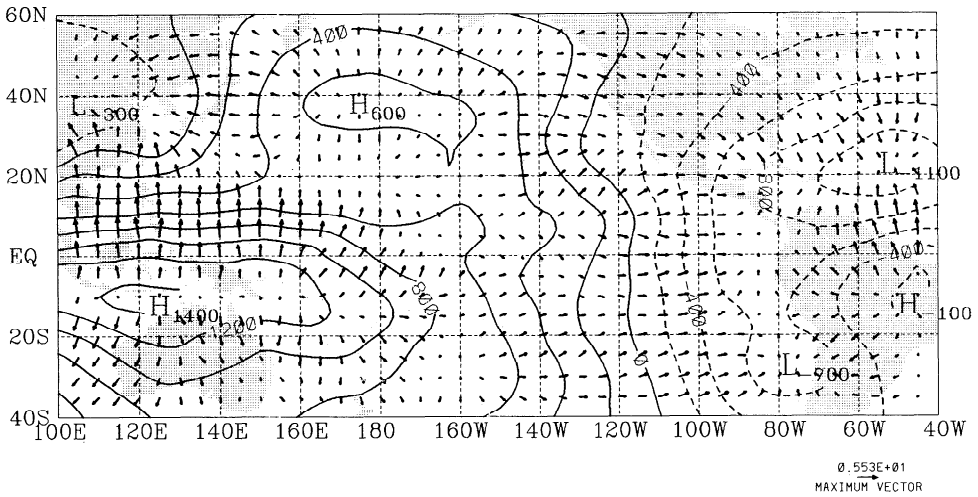

Figure 2b. Mean PEMWB velocity potential (units, 10^4 m^2 s^{-1}) and divergent wind (units, ms^{-1}) at 200 hPa.

water vapor mixing ratios ascending from below centered near 12°N, 150°E; 10°N, 80°W; and 7°N, 160°W in regions which correspond to convergence at 1000 hPa and divergence at 200 hPa (cf. Figure 1). The plume at 7°N, 160°W shows best on the vertical motion map of Figure 3a. The moist plume from Panama extends a considerable distance to the west, and there are also indications of an extension to the northeast into the Atlantic. There is also good correspondence between the high values of water vapor in the SPCZ region, the North Pacific near 160°W, and the velocity potential ridges at 200 hPa. The lowest values of H_2O mixing ratio in the tropics at 215 hPa occur at about 12°S, 120°W and 30°S, 80°W, almost exactly coincident with the minima in the velocity potential at 200 hPa. In the northern hemisphere, there is a tongue of dry air off California at about 120°W, extending southwestward, also in a region of convergence and sinking motion. A similar dry tongue extends northwestward from Chile toward the equator.

MLS results for the PEMWB period (Figures 4c and 4d) show the maximum H_2O mixing ratio to be at about 10°S, north of Australia and extending eastward, and another, almost as large, over Brazil; these areas correspond to the upward vertical motion patterns and the divergence pattern at 200 hPa. There is a secondary H_2O mixing ratio maximum at about 12°N, 125°W, while the maximum velocity divergence is at about 5°N. There are, however, few radiosonde data in that region. Moist values in the region to the east of Australia fit quite well with the SPCZ, as seen in Figure 2b. There are dry regions just south of the equator at about 90°W to 150°W. These correspond to sinking motion at 300 hPa (Figure 3b) and to convergence in the velocity field at 200 hPa at about 2°S (Figure 2b). Water vapor shows strong evidence that a plume extends west-southwestward from 10°S over South America to about 25°S, 95°W, suggesting considerable interactions between continental and marine air in that region. The extension of the continental outflow to the oceanic region shown by MLS is greater than that shown by the divergent wind pattern (cf. Figures 4c and 2b). Again, as there are practically no radiosonde data in that region and ECMWF was not using UARS data at this time, the water vapor

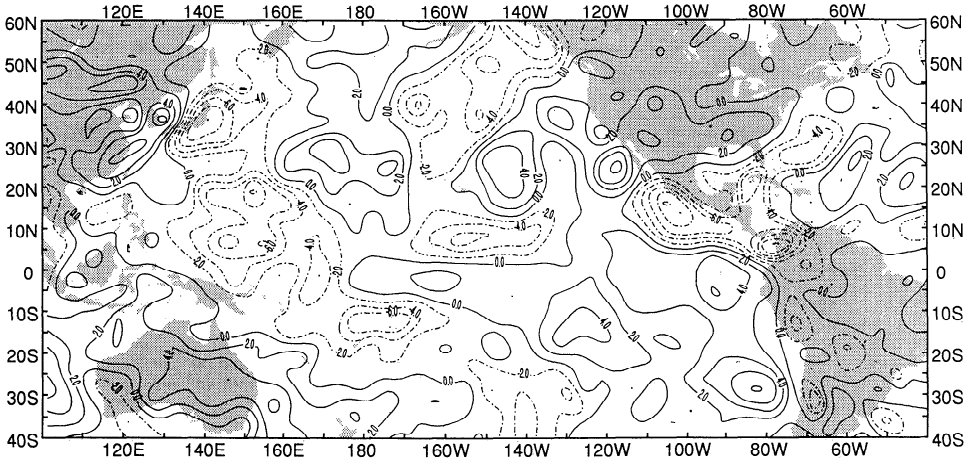

Figure 3a. Mean PEMWA vertical velocity at 300 hPa (units, 10^{-2} Pa s^{-1}).

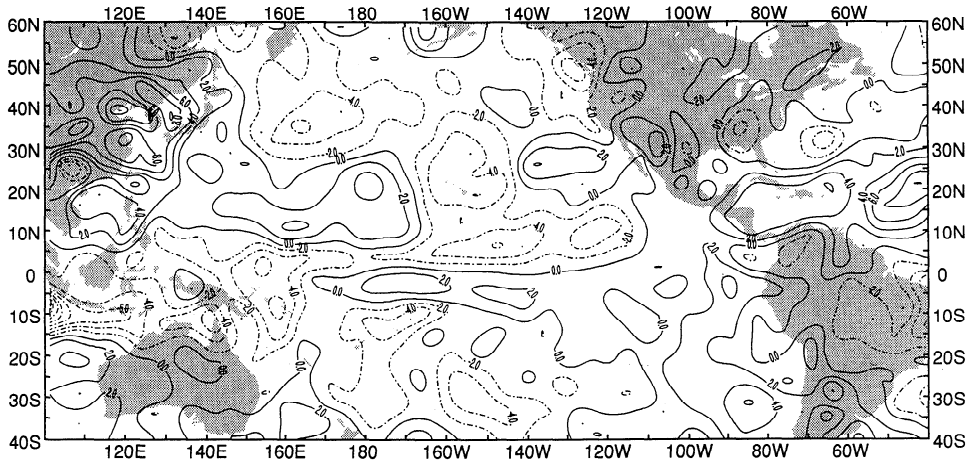

Figure 3b. Mean PEMWB vertical velocity at 300 hPa (units, 10^{-2} Pa s^{-1}).

tracer is probably giving the most reliable indication of the flow.

Overall, there is good agreement between water vapor, velocity potential, and vertical velocity patterns. As noted above, the addition of upper tropospheric water vapor to these studies gives a considerable improvement in delineating downstream plumes. Why the SPCZ has the observed form and why the orientation relative to the equator changes with season are dynamical questions not studied here, but it is noteworthy that the dry air on each side of the SPCZ is consistent with subsidence. The vertical motions of the Walker circulation are not completely toroidal, particularly in the PEMWA period, when the moist air associated with rising motion at 215 hPa is at ~12°N, 150°E, while the dry air associated with sinking motion occurs in a trough oriented ESE in the south-east Pacific. If water vapor alone is used as a tracer, then the 215 hPa map suggests that the west-east connection occurs only through the ESE orientation in the SPCZ (cf. Figures 1b and 4a). In the PEMWB period the rising motion occurs in the west Pacific mostly south of the equator, though there is some in the North Pacific; sinking motion occurs in the east Pacific in the lower troposphere, while in the upper troposphere off the west coast of South America, there is considerable influence of continentally derived air according to the water vapor maps.

Horizontal Linkage in the Walker Circulation

While the vertical motion components of the Walker circulation are easy to see in the velocity potential, divergent winds, and water vapor patterns, the horizontal components are more difficult to detect. In early climatologies they were brought out by taking deviations of zonal wind at a particular longitude from the zonal average of the zonal wind [*Newell et al.*, 1974]. Inspection of the rotational wind components (the largest wind component; see Figures 5a, 5b, 6a and 6b) shows that at 1000 hPa, easterlies are present in the eastern Pacific south of the equator in both periods but are not present in the western Pacific in PEMWA (Figure 5a) and extend to

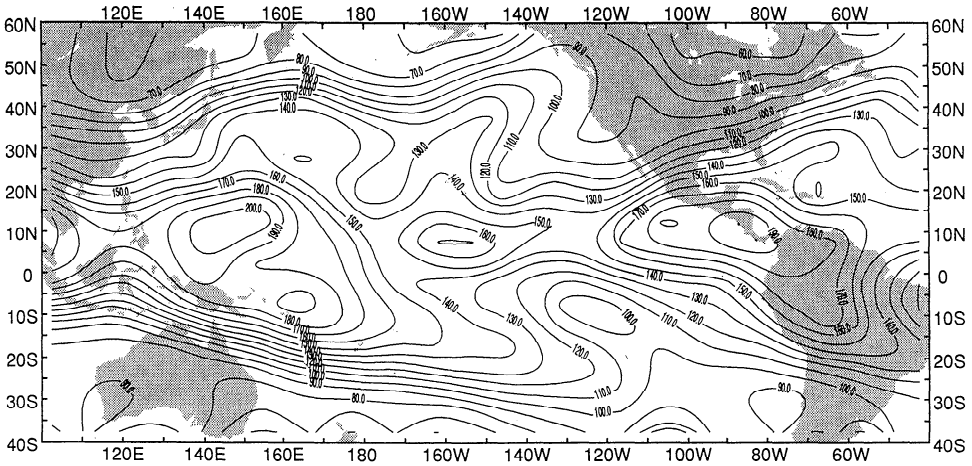

Figure 4a. Mean PEMWA microwave limb sounder (MLS) water vapor mixing ratio at 215 hPa (units, parts per million by volume (ppmv)).

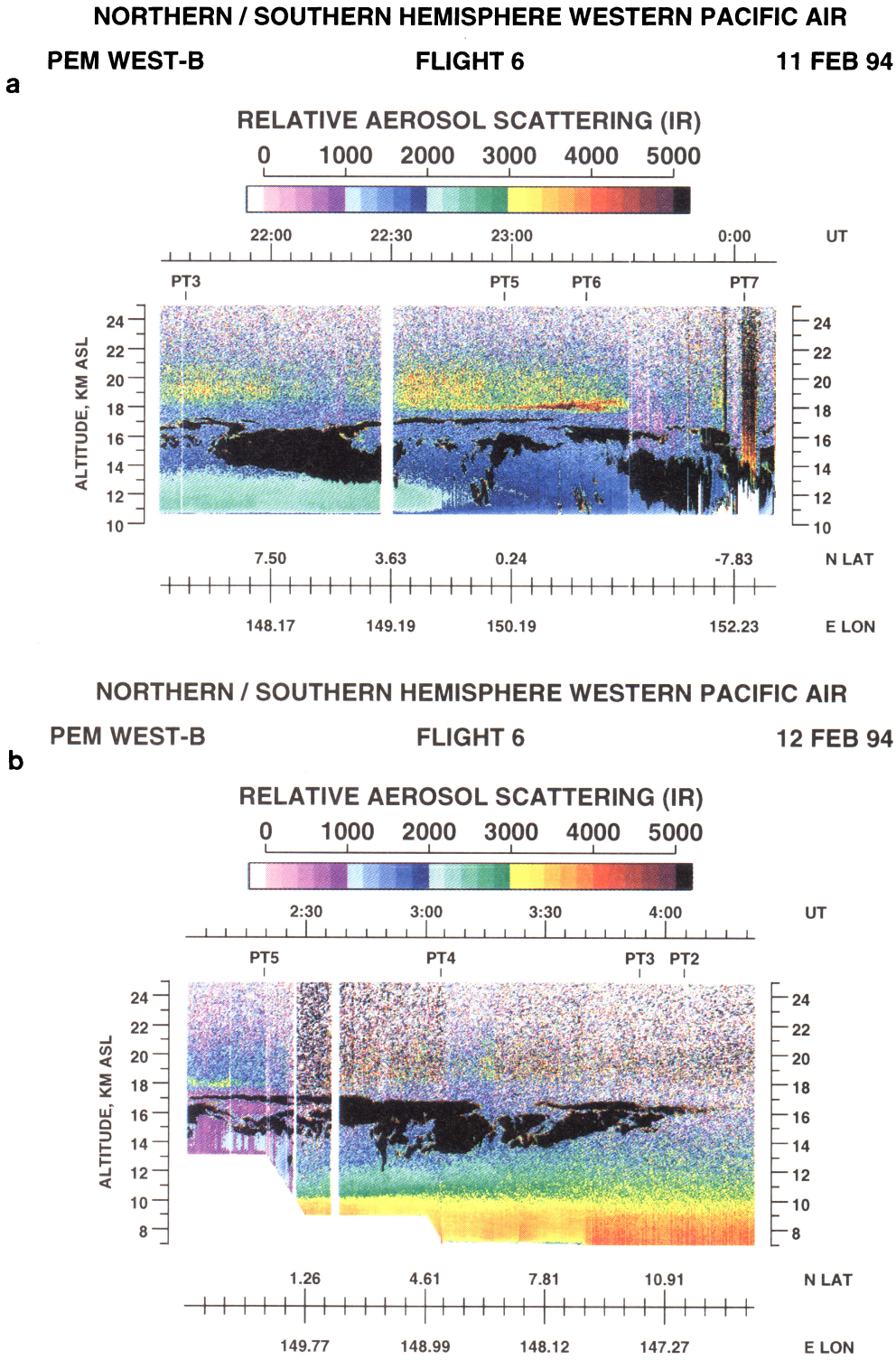

Plate 1. Examples of cirrus lidar cross sections from region to north of intertropical convergence zone: (a) February 11, 1994, 10°N to 8°S, 147°-152°E; (b) February 12, 1994, 0° to 13°N, 150-146°E; and (c) February 14, 1994, 17°N to 12°N along 147°E.

about 170°E both south and north of the equator in PEMWB (Figure 6a), continuing north of 5°N to the Asian continent. At 200 hPa near the equator, there are easterlies across the entire Pacific in PEMWA (Figure 5b), while in PEMWB (Figure 6b), they only cover the western Pacific. There is a westerly flow south of the equator east of 140°W, related to cross-equatorial flow near 140°W and subtropical westerly flow farther north. Thus there is no direct evidence for the horizontal arm of a Walker circulation connecting the western to the eastern tropical regions at 200 hPa in PEMWA, while the connection occurs via the equator in PEMWB, although there is a direct

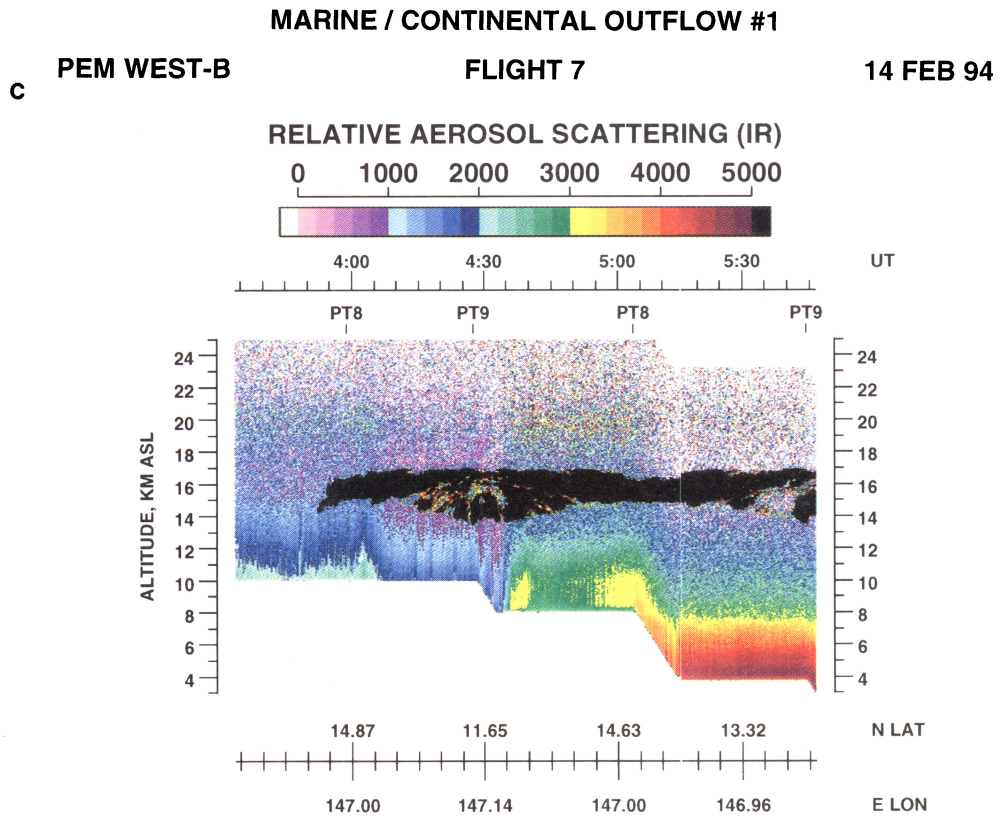

Plate 1. (continued)

link from China to Hawaii to North America in the subtropics. The same conclusions are reached from the mean wind vector field at 200 hPa (Figures 7 and 8), namely, that the evidence of a westerly wind component in the equatorial region only occurs in PEMWB east of the date line.

Evidence of the flow into the northern hemisphere upper troposphere from convective complexes south of the equator is given in the lidar images of cirrus clouds in Plate 1 that were taken from the DC-8 flying missions from Guam; these may be compared with the mean 200-hPa flow patterns seen in Figure 8, which show a drift toward the northwest. This site is too far west to be used to provide evidence of flow between the rising motion in the West Pacific and the sinking motion in the east. These images show that the main cirrus clouds, originating from the lower-level convergence zone near 10°S, have tops near the tropopause (as judged from the ozone lidar images) at 17-18 km. However, above the tropopause the broad aerosol layer in the 18 to 22-km height range is probably volcanic aerosols, thought to be from the 1991 Pinatubo eruption; this identification as volcanic is based on their scattering signature.

Evidence of Walker Circulation in the Mass Budget

The mass budget of two grid squares, 4444 km on a side (40° at the equator), centered on the rising motion region at 12°N, 140°E in PEMWA and 10°S, 140°E in PEMWB and two more centered on the sinking motion region at 30°S, 88°W in PEMWA and 30S, 83°W in PEMWB, has been evaluated from the divergent wind component used above. Mass flux across the western, eastern, southern, and northern boundaries is shown in Table 1. In the western cell the flux was integrated separately for the flow below and above 500 hPa, while 600 hPa was used as the pressure boundary for the eastern cell. Mass balance is not expected because the fluxes are derived from analyses of velocity potential and stream functions evaluated over a much larger area than the grids used here.

In the rising motion region, the main mass flux entering the grid was across the eastern and southern boundaries in PEMWA and across the northern, southern, and eastern boundaries in PEMWB, though in the latter case flux across all four boundaries is important. In the sinking motion region in the East Pacific, there is significant material entering the upper levels from all four boundaries in PEMWA, while in PEMWB, entry from the west predominates with significant amounts also across the eastern and southern boundaries. Apart from the substantial gain to the eastern cell from the west in PEMWB, these fluxes do not show evidence of a linkage between the rising arm of the Walker circulation in the West Pacific and its sinking arm in the East Pacific, as noted previously from the rotational wind components.

Exchange With the Stratosphere

Maps of 100-hPa temperature for PEMWA and PEMWB (not shown) show that lowest temperatures occurred in the western cell in PEMWB south of the equator. This area and season are thought to be preferred for the passage of

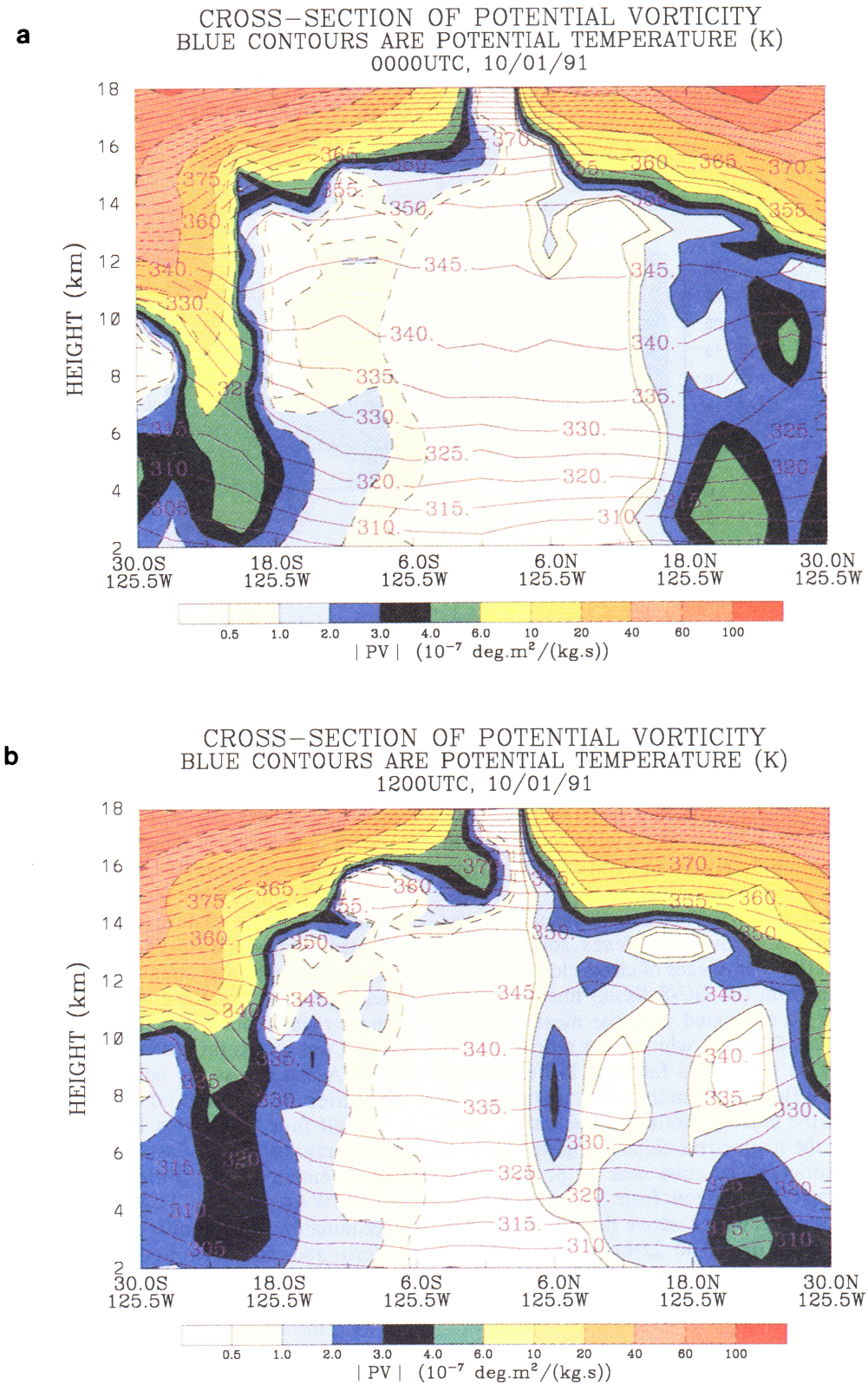

Plate 2. Cross sections of potential vorticity along 125°W on October 1, 1991. The plume at 6°N, 125°W shows UARS H_2O mixing ratios at 215 hPa of about 65 ppmv. Dashed lines represent negative potential vorticity, characteristic of the southern hemisphere. Units, 10^{-7} K m^2 kg^{-1} s^{-1}. (a) 0000 UT; (b) 1200 UT.

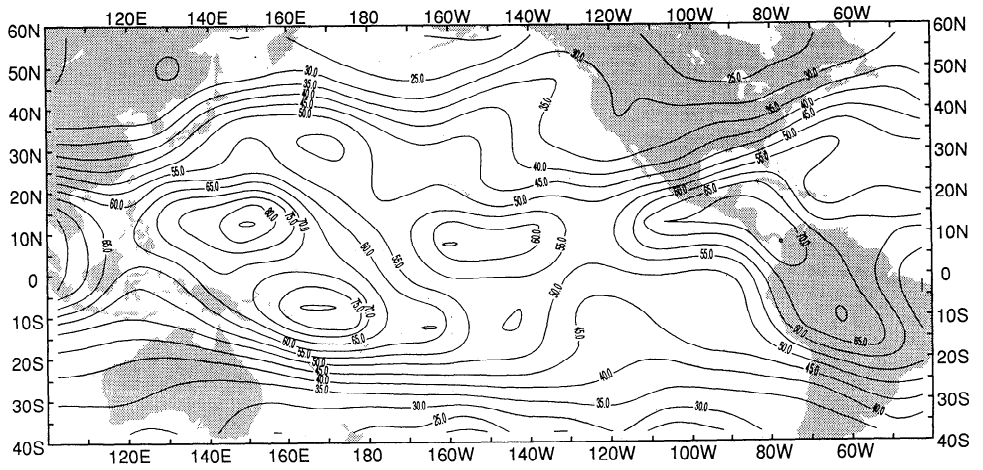

Figure 4b. Mean PEMWA MLS water vapor mixing ratio at 147 hPa (units, ppmv).

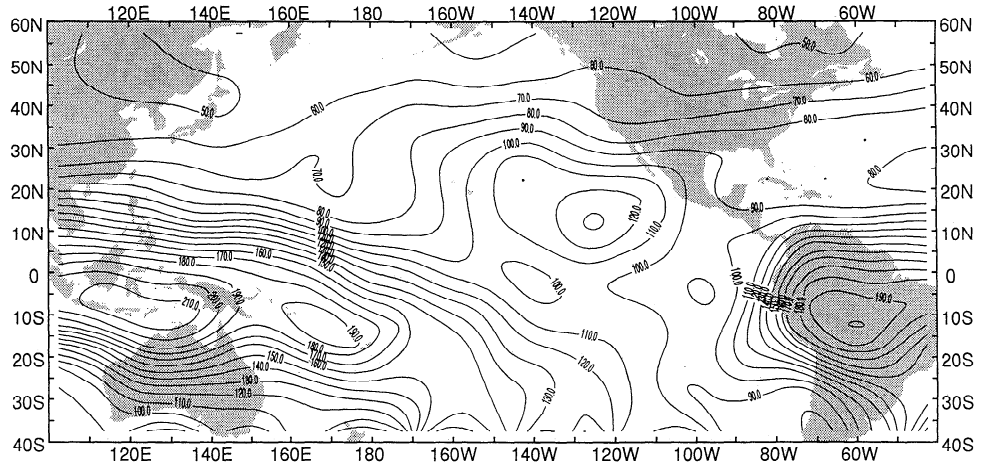

Figure 4c. Mean PEMWB MLS water vapor mixing ratio at 215 hPa (units, ppmv).

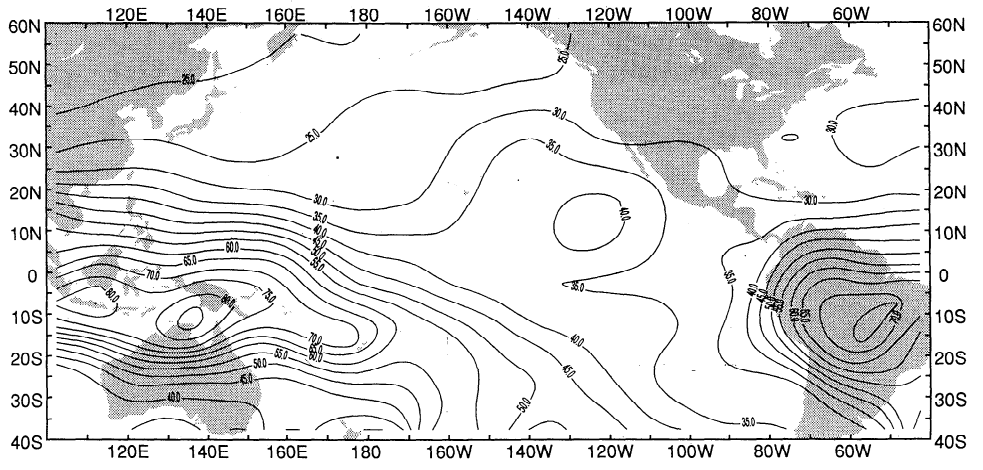

Figure 4d. Mean PEMWB MLS water vapor mixing ratio at 147 hPa (units, ppmv).

air into the stratosphere [*Newell and Gould-Stewart*, 1981]; the rising motion in the upper troposphere is thought to extend into the stratosphere, although the fraction associated with individual convective events relative to that which may be associated with a more general rising motion is not known. *Danielsen* [1993] has reported high-flying aircraft measurements that show direct evidence of convcctive events reaching into the stratosphere. A question that frequently is raised about the eastern tropical Pacific is whether there is sinking motion above the eastern

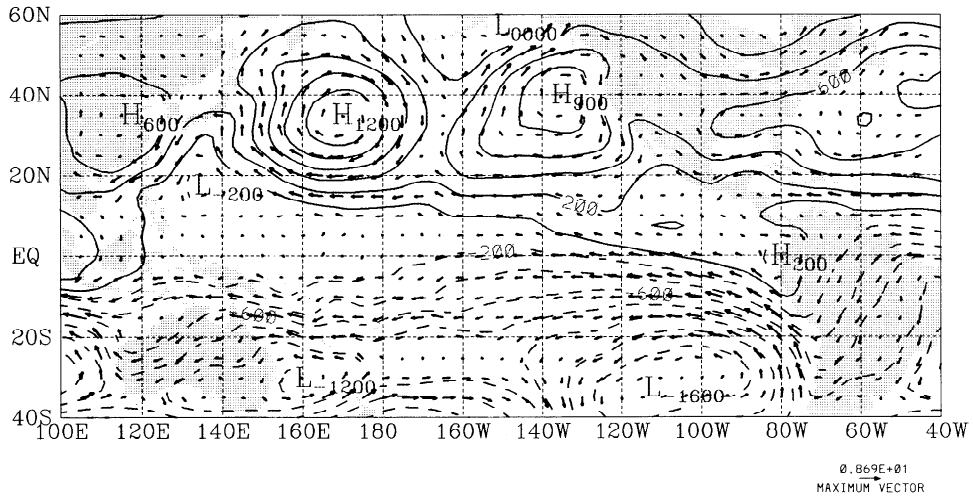

Figure 5a. Mean PEMWA stream function (units, 10^4 m^2 s^{-1}) and rotational wind (units, ms^{-1}) at 1000 hPa.

cell which may carry stratospheric material down into the upper troposphere. Daily maps of water vapor mixing ratio at 147 and 215 hPa have been examined for relatively dry air, and such regions have been found over the eastern Pacific above the sinking regions similar to conditions in the mean maps of Figures 1b, 2b and 4. Potential vorticity (PV) cross sections and maps have shown that some of the dry regions are accompanied by relatively high values in the form of plumes appearing to descend almost vertically from the lower stratosphere. An example is illustrated by two potential vorticity cross sections for October 1, 1991, in Plates 2a and 2b. The divergent wind component maps drawn for each 12-hour period show convergent winds in the dry regions at 200 hPa, and a vertical motion cross section (Figure 9) shows sinking motion at 6°N, in the same region as the high PV in Plate 2b. These velocity and PV cross sections show also a region of sinking motion and high PV at about 20°S, which is a well-known phenomenon. The question raised as to whether stratospheric air is involved in the sinking region with high PV at 6°N cannot be answered with the relatively poor coverage of radiosonde stations in this area. There is always the possibility that some of these features are advected into the tropics from middle latitudes. Elsewhere we report a census carried out for the entire tropical region, 15°N to 15°S, using daily water vapor maps and daily PV maps and cross sections for the two periods studied here. The phenomenon is also evident in the sinking arm of the Walker circulation that spans the region between South America and the South Atlantic and the sinking arm of the Hadley circulation that occurs over Australia in the PEMWA period. *Gage et al.* [1991], using wind-profiling Doppler radar, found evidence of a "reverse" Walker circulation in the lower stratosphere with rising motion in the central Pacific above the tropospheric sinking motion. On the other hand, *Smit et al.* [1990] reported plumes of dry air in the upper troposphere in the tropical Atlantic which are ozone rich, suggesting a stratospheric source. It would be valuable if ozone measurements were made with a high-flying aircraft in the eastern Pacific [see *Browell et*

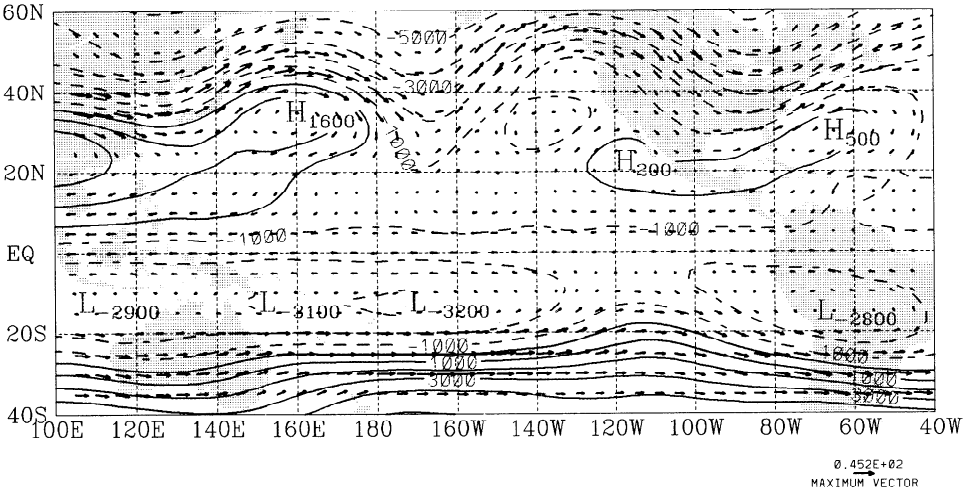

Figure 5b. Mean PEMWA stream function (units, 10^4 m^2 s^{-1}) and rotational wind (units, ms^{-1}) at 200 hPa.

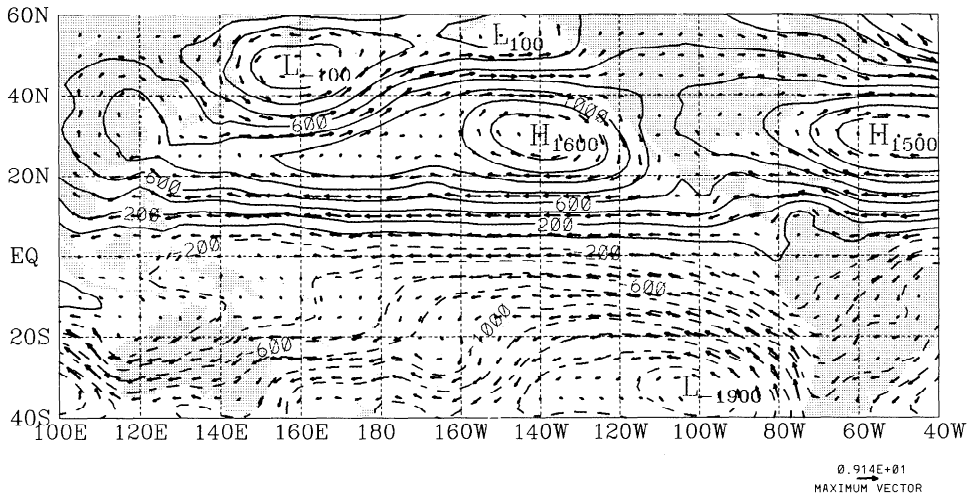

Figure 6a. Mean PEMWB stream function (units, 10^4 m^2 s^{-1}) and rotational wind (units, ms^{-1}) at 1000 hPa.

al., this issue]. Alternatively, water vapor lidars could be used to search for very dry air near the tropopause in that region. There is clearly more experimental and diagnostic work to be performed on the topic of tropospheric-stratospheric exchange in the tropics.

Conclusions

1. Divergent wind patterns derived from ECMWF analyses show, as expected, the rising arm of the Walker circulation in the West Pacific and the sinking arm in the Southeast Pacific, but the rotational wind components or streamlines do not show evidence of a direct tropical link between the east and the west in the PEMWA period at 200 hPa and only evidence of an indirect link from the northern subtropics across the equator in the PEMWB period.

2. In October 1991 the inflow to the sinking arm of the Walker circulation in the Southeast Pacific includes a significant contribution from continental outflow as well as from the northern hemisphere; in February 1994 the largest inflow is from the west, but a slightly greater mass flux comes in from the east and south combined.

3. Water vapor data at 215 hPa and 147 hPa fit with the divergent wind field pattern in PEMWA, showing moist plumes in the West Pacific, along the SPCZ region, over Panama and over the tropical central Pacific with a generally dry region in the East Pacific outside the tropics. The water vapor data show more details of the flow patterns than can be gained from the velocity potential maps with the moist plumes extending to the northeast across the North Pacific, to the ESE across the South Pacific, and to the west from Panama in the PEMWA period. In the PEMWB period the water vapor maps show good evidence of flow out of South America at 215 hPa, extending almost to 100°W, considerably farther than is evident from the meteorological analysis.

4. Lidar images of cirrus show good evidence of interhemispheric flow northward just below the tropopause from ~10°S in PEMWB.

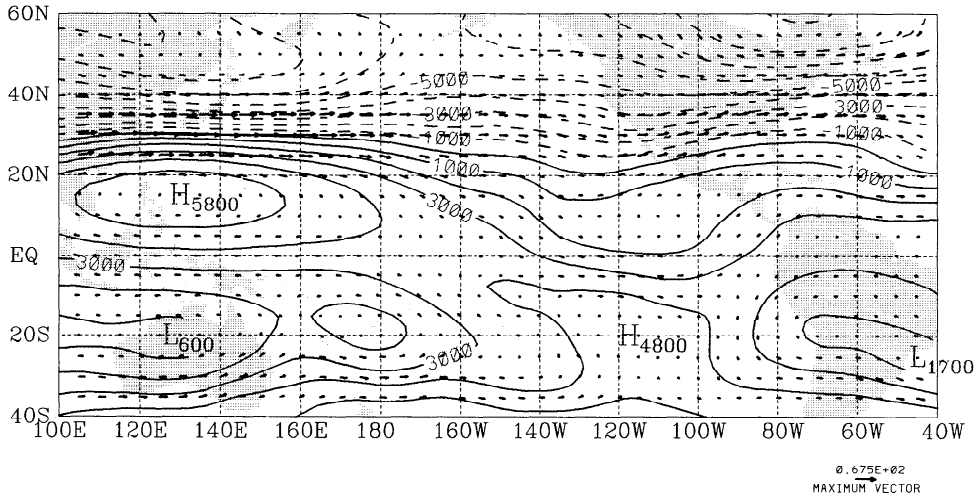

Figure 6b. Mean PEMWB stream function (units, 10^4 m^2 s^{-1}) and rotational wind (units, ms^{-1}) at 200 hPa.

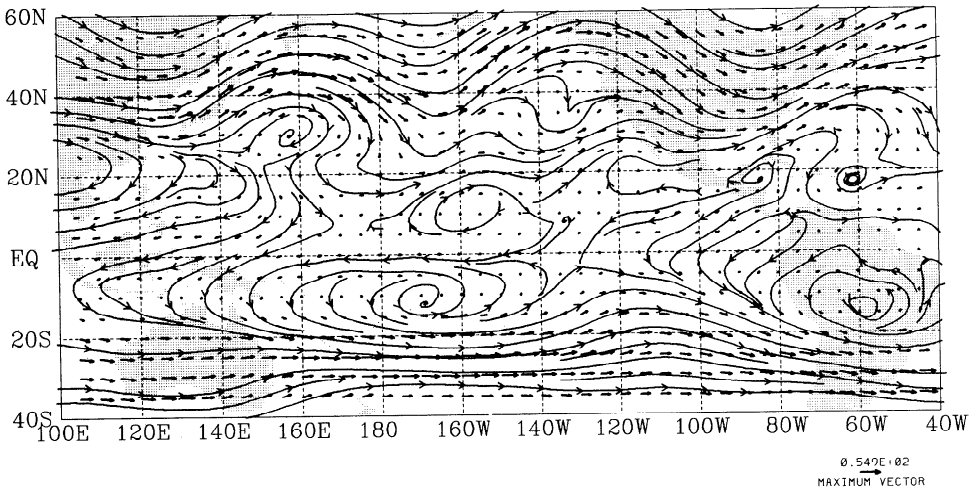

Figure 7. Mean PEMWA streamlines and wind vectors (units, ms^{-1}; see scale in bottom right-hand corner) for Pacific at 200 hPa.

5. Daily maps of water vapor from UARS showed small-scale patches of dry air at 215 hPa in the tropics that were generally accompanied by convergence in the upper troposphere and sometimes by plumes of high potential vorticity seeming to penetrate from the stratosphere into the upper troposphere. These are being investigated further; aircraft sampling would clearly be helpful in examining possible linkages.

6. The western branch of the Walker circulation has been examined during the PEM-West atmospheric chemistry experiments. The eastern branch promises to be equally interesting, and as for PEM-West, chemistry experiments are expected to improve our knowledge of the circulation there. It would be desirable to make aircraft sorties, including vertical profiles, along the west coast of South America to examine the continental outflow and sorties along the equator to examine the flow from the northern hemisphere. Sorties along the western and southern boundaries of the southeastern Pacific cell and also in the tropopause region would complete the information needed to study chemical budgets. These sorties would benefit from lidar measurements of ozone, aerosol, and water vapor.

To examine the ozone budget of this sinking arm of the Walker circulation, it would be desirable to set up an ozonesonde station on each of four boundaries; there are radiosonde stations at Galapagos, Lima, Easter Island, and Papeete which could be used in such an investigation.

To check for material entering the region from the stratosphere, whether directly or indirectly from middle latitudes, a high-flying aircraft able to penetrate the tropopause would be desirable. Because of the lack of basic meteorological information in the Southeast Pacific region, which must be reflected to some extent in the available analyses, it is expected that detailed aircraft measurements associated with atmospheric chemistry sampling and continued UARS data will provide a new perspective on the meteorology of the region.

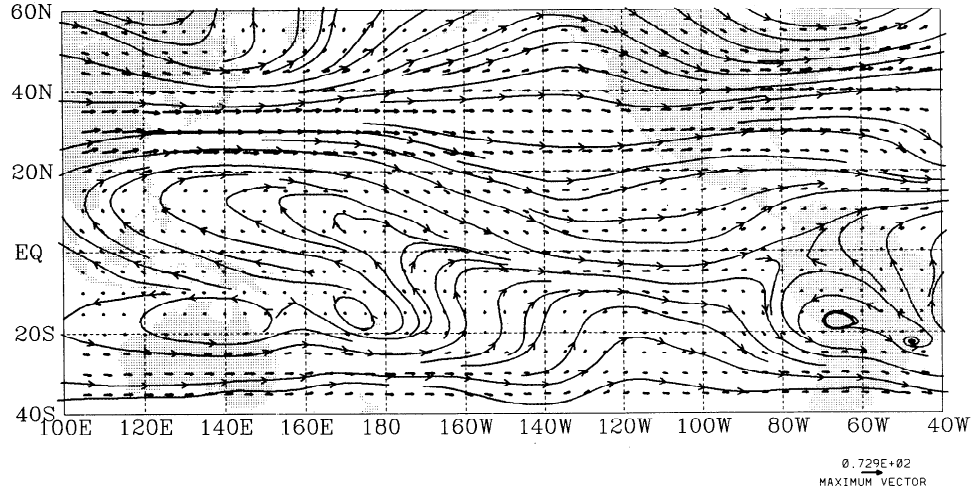

Figure 8. Mean PEMWB streamlines and wind vectors (units, ms^{-1}; see scale in bottom right-hand corner) for Pacific at 200 hPa.

Table 1. Mass Flux in 10^9 kg s^{-1} Across Boundaries of Grid Square Centered as Indicated

	Western Cell 12°N, 140°E					Eastern Cell 30°S, 88°W			
Layer, hPa	W	E	S	N	Layer, hPa	W	E	S	N
				PEMWA					
500-100	-6	-8	-27	-14	600-100	13	11	11	14
		net outflow = 55					net inflow = 49		
1000-500	2	18	26	12	1000-600	-5	3	-4	-13
		net inflow = 60					net outflow = 19		
	Western Cell 10°S, 140°E					Eastern Cell 30°S, 83°W			
	W	E	S	N		W	E	S	N
				PEMWB					
500-100	-13	4	-20	-33	600-100	24	11	17	-3
		net outflow = 70					net inflow = 49		
1000-500	11	17	18	34	1000-600	-9	-1	-10	3
		net inflow = 80					net outflow = 17		

Positive values represent inward flow.

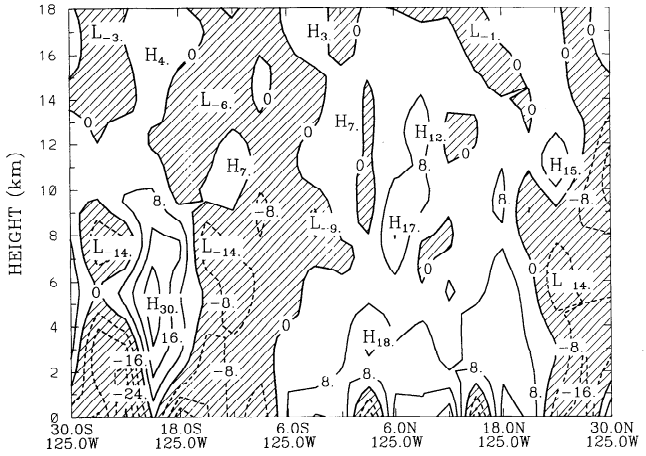

Figure 9. Cross section of vertical motion for 125°W on October 1, 1991, from the European Center for Medium-Range Weather Forecasts data. Units, 10^{-2} Pa s^{-1}.

Acknowledgments. The work was supported under NASA grant 1-1252. We thank the European Center for Medium-Range Weather Forecasts for their provision of grid point data for both the PEMWA and the PEMWB missions.

References

Barath, F.T., et al., The Upper Atmosphere Research Satellite microwave limb sounder instrument, *J. Geophys. Res., 98*, 10,751-10,762, 1993.

Bjerknes, J., Atmospheric teleconnections from the equatorial Pacific, *Mon. Weather Rev., 97*, 163-172, 1969.

Bluestein, H.B., *Synoptic-dynamic meteorology, in Midlatitudes*, vol. II, p. 175, Oxford Univ. Press, New York, 1993.

Browell, E.V. et al., Large-scale air mass characteristics observed over the western Pacific during the summertime, *J. Geophys. Res.*, this issue.

Danielsen, E.F., In situ evidence of rapid, vertical, irreversible transport of lower tropospheric air into the lower tropical stratosphere by convective cloud turrets and by larger-scale upwelling in tropical cyclones, *J. Geophys. Res., 98*, 8665-8681, 1993.

Gage, K.S., J.R. McAfee, D.A.Carter, W.L. Ecklund, A.C. Riddle, G.C. Reid, and B.B. Balsley, Long-term mean vertical motion over the Tropical Pacific: Wind-profiling Doppler radar measurements, *Science, 254*, 1771-1773, 1991.

Heastie, H., and P.M. Stephenson, *Upper Winds Over the World, Geophys. Mem. 13* (103), 217 pp., G. B. Meteorol. Office, London, 1960.

Hoell, J.M., D.D. Davis, S.C. Liu, R.E. Newell, M. Shipham, H. Akimoto, R.J. McNeal, R.J. Bendura, and J.W. Drewry, The Pacific Exploratory Mission-West A (PEM-West A): September-October 1991, *J. Geophys. Res.*, this issue.

Newell, R.E., and S. Gould-Stewart, A stratospheric fountain?, *J. Atmos. Sci., 38*, 2789-2796, 1981.

Newell, R.E., J.W. Kidson, D.G. Vincent, and G.J. Boer, *The General Circulation of the Tropical Atmosphere*, vol. 2, pp. 143-178, MIT Press, Cambridge, Mass., 1974.

Newell, R.E., Y. Zhu, E.V. Browell, S. Ismail, W.G. Read, J.W. Waters, K.K. Kelly, and S.C. Liu, Upper tropospheric water vapor and cirrus: Comparison of DC-8 observations, UARS microwave limb sounder measurements and meteorological analyses, *J. Geophys. Res.*, this issue.

Philander, S.G., *El Niño, La Niña, and the Southern Oscillation*, Academic, 289 pp., San Diego, Calif., 1990.

Smit, H.G.J., S. Gilge, and D. Kley, The meridional distribution of ozone and water vapor over the Atlantic

Ocean between 30°S and 52°N in September/October, in *Physicochemical Behavior of Atmospheric Pollutants*, edited by G. Restelli and G. Angeletti, Nowell, Mass., pp. 630-637, Kluwer Academic, 1990.

Troup, A.J., The 'southern oscillation,' *Q. J. R. Meteorol. Soc.*, *91*, 490-506, 1965.

Weatherburn, C.E., *Advanced Vector Analysis*, pp. 44-45, C. Bell and Sons, London, 1951.

E. V. Browell, NASA Langley Research Center, Mail Stop 401A, Hampton, VA 23681-0001. (e-mail: e.v. browell@larc.nasa.gov).

R. E. Newell (corresponding author) and Y. Zhu, Department of Earth, Atmospheric and Planetary Sciences, Massachusetts Institute of Technology, 77 Massachusetts Avenue, Room 54-1824, Cambridge, MA 02139. (e-mail: newell@newell1.mit.edu; zhu@newell1.mit.edu).

W. G. Read and J. W. Waters, Jet Propulsion Laboratory, Mail Stop 183-701, 4800 Oak Grove Drive, Pasadena, CA., 91109

(Received January 11, 1995; revised June 24, 1995; accepted June 24, 1995.)